

Cholesterol stiffening of lipid membranes and drug interactions: Insights from neutron spin echo and deuterium NMR spectroscopy

Sudipta Gupta^{a,*}, Fathima T. Doole^{b,*}, Teshani Kumarage^a,
Milka Doktorova^c, George Khelashvili^{d,e}, Rana Ashkar^a,
and Michael F. Brown^{b,f}

^aDepartment of Physics and Center for Soft Matter and Biological Physics, Virginia Tech, Blacksburg, VA, United States ^bDepartment of Chemistry and Biochemistry, University of Arizona, Tucson, AZ, United States ^cDepartment of Molecular Physiology and Biological Physics, University of Virginia School of Medicine, Charlottesville, VA, United States

^dDepartment of Physiology and Biophysics, Weill Cornell Medical College, New York, NY, United States ^eInstitute of Computational Biomedicine, Weill Cornell Medical College, New York, NY, United States ^fDepartment of Physics, University of Arizona, Tucson, AZ, United States

Abbreviations

DMPC	1,2-dimyristoyl- <i>sn</i> -glycero-3-phosphocholine
DOPC	1,2-dioleoyl- <i>sn</i> -glycero-3-phosphocholine
EFG	electric field gradient
LUV	large unilamellar vesicles
MD	molecular dynamics
NMR	nuclear magnetic resonance
NSE	neutron spin echo
PC	phosphocholine or phosphatidylcholine
PE	phosphoethanolamine or phosphatidylethanolamine

* Both authors contributed equally to this work.

POPC	1-palmitoyl-2-oleoyl- <i>sn</i> -glycero-3-phosphocholine
POPC- <i>d</i> ₃₁	1-perdeuteriopalmityl-2-oleoyl- <i>sn</i> -glycero-3-phosphocholine
PS	phosphoserine or phosphatidylserine
SANS	small-angle neutron scattering
SAXS	small-angle X-ray scattering
ZG	Zilman and Granek

Introduction

Lipid bilayers form the main matrix of cell membranes and are the primary platform for nutrient exchange, protein–cell interactions, and viral budding, among other vital cellular processes. The intermolecular interactions at mesoscopic length scales play key roles in the emergence of membrane physical properties, such as lipid packing and membrane rigidity. The functioning of cell membranes leverages on their hierarchical dynamics encompassing segmental lipid fluctuations, molecular diffusion, and viscoelastic membrane deformation. Lipid membrane fluctuations correspond to the geometry of interactions and the rates of lipid motions as described by their order parameters and correlation times. These phospholipid mobilities occur at their own timescales, and various biophysical techniques can be utilized to monitor the different dynamics in terms of an energy landscape (Fig. 1).

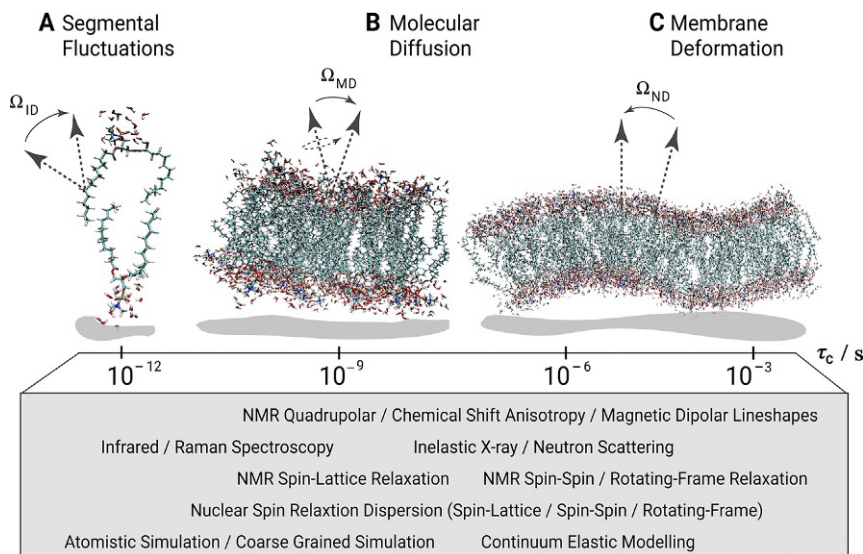


FIG. 1 Biophysical techniques reveal phospholipid membrane dynamics over a range of timescales. Orientational fluctuations correspond to the geometry of interactions via Euler angles Ω and correlation times τ_c for the rates of lipid motions. (A) Principal axis system of ^{13}C – ^1H or C – ^2H bonds fluctuate due to motions of internal segmental frame (I) with respect to the membrane director (D) axis. (B) Diffusive phospholipid motions are described by anisotropic reorientation of molecule-fixed frame (M) with respect to the membrane director axis (D) as described by Ω_{MD} Euler angles. (C) Liquid-crystalline bilayer lends itself to propagation of thermally excited quasi-periodic fluctuations in membrane curvature expressed by motion of the local membrane normal (N) versus membrane director axis (D) as described by Ω_{ND} Euler angles. Bottom part of the figure lists techniques that offer temporal resolution appropriate to capturing lipid and membrane dynamics events. Adapted from Leftin, A., & Brown, M. F. (2011). An NMR data base for simulations of membrane dynamics. *Biochimica et Biophysica Acta*, 1808, 818–839.

The major classes of membrane lipids are phospholipids, glycolipids, and sterols, with their representative chemical structures illustrated in Fig. 2. In cell membranes, lipids exist in various forms that differ in their polar head group size, charge, and capacity for hydrogen bonding, as well as in their nonpolar acyl chain length and degree of unsaturation (Fig. 2A–C). Phospholipids are the main components of the lipid bilayers of mammalian cells. The second most abundant component is cholesterol, constituting up to 50 mol% of the total lipids of the plasma membrane (Krause & Regen, 2014)—which has justifiably drawn significant attention in membrane biophysics over the last few decades. The fact that cholesterol is present in large amounts in mammalian cells but is absent in prokaryotic cells (Mouritsen & Zuckermann, 2004) indicates its important role in cell evolution. Its molecular fraction in different cell membranes is controlled through biosynthesis, efflux from cells, and influx of lipoprotein cholesterol into the cell (Simons & Ikonen, 2000). Functionally, cholesterol is involved in key biological processes such as cellular homeostasis, steroid and vitamin D synthesis, and the regulation of membrane order and dynamics (Craig, Yarrarapu, & Dimri, 2021). Therefore, changes in cholesterol level are commonly attributed to variations in membrane properties, stability, and pathology. There are two well-known methods that describe how cholesterol modulates cellular functions: (i) by indirectly affecting membrane properties and consequently influencing protein–membrane interactions (Brown, 1994, 2012, 2017), and (ii) by directly affecting cholesterol–protein interactions (Liu et al., 2017; Sheng et al., 2012).

Structurally, cholesterol is a 27-carbon compound characterized by a hydrocarbon tail, a central sterol nucleus made of four hydrocarbon rings, and a hydroxyl group (Fig. 2D) (Craig et al., 2021). This structure facilitates the incorporation of cholesterol into lipid membranes and its alignment along the hydrocarbon chains of the lipids (Fig. 2B and C). The orientation of cholesterol results in a more ordered state of the hydrocarbon chains, and consequently modulates the membrane structural, dynamical, and physical properties. In membranes with saturated and unsaturated lipids, cholesterol preferentially segregates into domains rich in saturated lipids, also known as lipid rafts, which may include glycolipids (Fig. 2E). These raft domains play an important role in cell signaling and pharmacology (Brown & London, 1998; Klose, Surma, & Simons, 2013; Simons & Gerl, 2010), as well as maintaining membrane order (Zhang, Barraza, & Beauchamp, 2018). Notably, the increase in lipid packing due to cholesterol can lower the membrane permeability, and it can affect the distribution and transport of anesthetics and other drugs in membranes (Auger, Jarrell, & Smith, 1988; Siminovitch, Brown, & Jeffrey, 1984). Therefore, cholesterol also plays a significant regulatory role in many biophysical processes (Maxfield & van Meer, 2010), including passive permeation (Corvera, Mouritsen, Singer, & Zuckermann, 1992), protein and enzyme activity (Cornelius, 2001; de Meyer, Rodgers, Willems, & Smit, 2010), and viral infections, e.g., influenza (Sun & Whittaker, 2003), HIV (Prasad & Bukrinsky, 2014), and coronavirus (Meher, Bhattacharjya, & Chakraborty, 2019).

Beside the central role of cholesterol in naturally occurring membrane processes, it also poses as a key component in drug development and drug delivery applications. For example, the presence of cholesterol in renal cell membranes is a critical factor in improving the membrane resistance against damage inflicted by nephrotoxic antibiotics (Khondker et al., 2017). This is attributed to increased membrane stabilization and suppression of lipid and peptide mobility imparted by cholesterol. Such modifications of membrane properties by cholesterol have also been utilized in the design of liposomal formulations, resulting in significant advances in the use of liposomes as drug carriers (Allen & Cullis, 2013). Specifically,

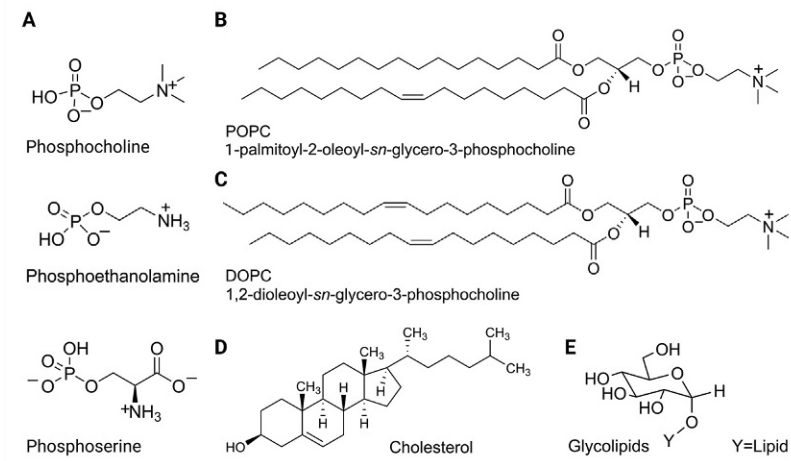


FIG. 2 There are three major classes of membrane lipids. Structures of (A) the polar lipid head groups vary in their size, capacity for hydrogen bonding, e.g., the zwitterionic phosphocholine (PC) and phosphoethanolamine (PE) head groups, and the anionic phosphoserine (PS) head group. Examples are shown for glycerophospholipids (B) POPC and (C) DOPC, (D) cholesterol, which is the sterol component of animal membranes, and (E) glycolipids with a carbohydrate moiety attached by a covalent bond.

the inclusion of cholesterol in liposomal membranes results in stable and long-circulating liposomes *in vivo*, a necessary feature for the protection of the drug cargo from degradation and premature release (Allen & Cullis, 2013; Leeb & Maibaum, 2018). In addition, cholesterol reduces the activity of proteins and peptides (part of the innate immune system) on liposomal bilayers (Zaslhoff, 2002), thus prolonging the liposome circulation time. Such findings point to the importance of cholesterol-induced modifications of membrane structural, dynamical, and mechanical properties in determining the efficacy of membrane-interacting drugs and in the developing of robust liposomal drug carriers.

To understand the effect of cholesterol on membrane mechanics, various techniques have been used, including flickering spectroscopy (Duwe, Kaes, & Sackmann, 1990), micropipette aspiration (Bassereau, Sorre, & Lévy, 2014; Dimova, 2014; Evans & Rawicz, 1990), electrodeformation (Gracià, Bezlyepkina, Knorr, Lipowsky, & Dimova, 2010; Niggemann, Kummrow, & Helfrich, 1995), X-ray diffusivity (Pan, Tristram-Nagle, & Nagle, 2009), molecular dynamics (MD) simulations (Doktorova, LeVine, Khelashvili, & Weinstein, 2019; Khelashvili & Harries, 2013; Khelashvili, Johner, Zhao, Harries, & Scott, 2014), deuterium nuclear magnetic resonance (^2H NMR) (Brown, Ribeiro, & Williams, 1983; Molugu & Brown, 2016), and neutron spin echo (NSE) spectroscopy (Arriaga et al., 2009; Chakraborty et al., 2020). Among these techniques, MD simulations, solid-state ^2H NMR and NSE spectroscopy uniquely access collective lipid fluctuations over length and time scales that are commensurate with fast biological processes, including protein–membrane interactions and signaling events. In this chapter, we discuss the powerful combination of solid-state ^2H NMR and NSE spectroscopy in non-invasively investigating membrane mechanics using spin labeling methods. In solid-state ^2H NMR, this approach involves studying the relaxation of deuterium spin labels along the hydrocarbon chain of the lipid molecules under the influence of a magnetic field. In NSE

spectroscopy, the experiments involve the change in spin polarization of an incident neutron beam as it exchanges energy with the measured lipid membrane. To illustrate the mode of operation of the two techniques, we summarize their basic principles and their use in studies of membrane fluctuations. Application to lipid bilayers give a powerful and unique approach to determining their mechanical or viscous membrane properties and how they emerge from atomistic-level forces that affect cholesterol- and drug-membrane interactions.

Neutron spin echo spectroscopy of lipid membranes

Neutron spin echo (NSE) spectroscopy is a high-resolution quasi-elastic scattering technique which measures neutron energy changes on the order of a few meV (or $k_B T$), making it ideally suited for directly detecting thermal fluctuations in lipid membranes. As mentioned above, the molecular motions of the lipids and their collective membrane dynamics are manifested over a broad range of length and time scales. For the length scales accessible by NSE, i.e., 1–100 nm, the membrane dynamics include collective lipid motions such as bending undulations (asymmetric deformations), breathing modes (symmetric deformations), as well as diffusive lipid dynamics (Gupta, De Mel, & Schneider, 2019; Katsaras & Gutberlet, 2001; Woodka, Butler, Porcar, Farago, & Nagao, 2012). Importantly, the bilayer physical chemistry underlies both molecular fluctuations and collective membrane dynamics (Brown et al., 1983). Thus, the ability to measure different membrane dynamics is crucial to understanding the fundamental biophysical properties of cell membranes, developing next generation biomaterials and extending our knowledge beyond the capabilities of current theory or simulations. Neutron spin echo spectroscopy has proven to be particularly valuable in accessing selective membrane dynamics over well-defined spatial and temporal scales, helping answer a number of open questions in membrane biophysics as discussed in the subsequent sections (Ashkar et al., 2015; Chakraborty et al., 2020; Gupta et al., 2018; Nagao, Kelley, Ashkar, Bradbury, & Butler, 2017; Woodka et al., 2012).

Neutron spin echo principles

Neutron spin echo spectroscopy measures the dynamic structure factor $S(\mathbf{Q}, t)$ as a function of momentum transfer vector, \mathbf{Q} , and Fourier time, t , the latter of which can vary up to several hundred nanoseconds. For a system composed of N_p nuclei of type α and β , the dynamic structure factor is defined as:

$$S_{\alpha,\beta}(\mathbf{Q}, t) = \frac{1}{N_p} \int d\mathbf{r} G_{\alpha,\beta}(\mathbf{r}, t) \exp(i\mathbf{Q} \cdot \mathbf{r}) \quad (1)$$

where $G_{\alpha,\beta}(\mathbf{r}, t)$ represents the density-density pair-correlation or the Van Hove function (van Hove, 1954) at different times and is given by:

$$G_{\alpha,\beta}(\mathbf{r}, t) = \int d\mathbf{R} \rho_{\alpha}(\mathbf{R} + \mathbf{r}, t) \rho_{\beta}^*(\mathbf{R}, 0) \quad (2)$$

It describes the probability of finding a nucleus of type α at Fourier time t at a distance $\mathbf{R} + \mathbf{r}$ if another particle of type β was at position \mathbf{R} at time 0. Another feature of NSE is the ability to directly measure the intermediate scattering function $S(\mathbf{Q}, t)$ as the Fourier transform of $S(\mathbf{Q}, \omega)$, i.e.,

$$S_{\alpha, \beta}(\mathbf{Q}, \omega) = \int_{-\infty}^{+\infty} dt S_{\alpha, \beta}(\mathbf{Q}, t) \exp(-i\omega t) \quad (3)$$

However, because of the two-third probability of spin-flip for spin incoherent scattering on NSE spectrometers, we measure the normalized total signal as:

$$\frac{I(\mathbf{Q}, t)}{I(\mathbf{Q}, 0)} = \frac{S(\mathbf{Q}, t)}{S(\mathbf{Q}, 0)} = \frac{\sigma_{\text{coh}} S_{\text{coh}}(\mathbf{Q}, t) - \frac{1}{3} \sigma_{\text{inc}} S_{\text{inc}}(\mathbf{Q}, t)}{\sigma_{\text{coh}} S_{\text{coh}}(\mathbf{Q}, 0) - \frac{1}{3} \sigma_{\text{inc}} S_{\text{inc}}(\mathbf{Q}, 0)} \quad (4)$$

Here, $S_{\text{coh}}(\mathbf{Q}, t)$ and $S_{\text{inc}}(\mathbf{Q}, t)$ correspond to the coherent and incoherent intermediate scattering functions, and σ_{coh} and σ_{inc} are the coherent and incoherent scattering cross-sections which depend on the neutron scattering length, b , of scattering nuclei, as $\sigma_{\text{coh}/\text{inc}} = 4\pi b_{\text{coh}/\text{inc}}^2$. We note that the remarkably distinct neutron scattering lengths of protium and deuterium isotopes of hydrogen (-3.74 fm and $+6.67$ fm, respectively) present a unique capability in biological sciences (Ashkar et al., 2018). Indeed, this difference in scattering length enables the visualization of different moieties in biological systems through simple substitution of hydrogen (or protium) with deuterium.

Neutron spin echo technique

Neutron spin echo (NSE) spectrometers probe sample dynamics by using neutron spin coding to measure the energy exchange between neutrons and the sample during scattering events. The Larmor precession of the neutron spin, within the magnetic coils of the spectrometer, serves as a timer for each neutron and allows the detection of tiny velocity changes ($\Delta v/v < 10^{-5}$) in a scattering event, measured as a change in the final beam polarization (Mezei, 1972; Mezei, Pappas, & Gutberlet, 2002; Monkenbusch & Richter, 2007).

The schematic setup of an NSE instrument can be seen in Fig. 3. Neutrons enter the instrument after passing a velocity selector that admits a velocity distribution with a width of 10% to 20%. Since the spin is used as a timer for each individual neutron, the initial velocity is of no importance for the actual measurement of the energy transfer, which facilitates the use of a broad-wavelength band of incident neutron energies. The incoming neutron beam is polarized by using a magnetic multilayer mirror which aligns the spins along the direction of the beam (x -direction). A $\pi/2$ flipper then flips the spin in the direction perpendicular to the beam axis, i.e., upwards (z -direction). Spin flippers work by applying a sharp magnetic field change to reorient the neutron spin. After passing the $\pi/2$ flipper, the neutron enters the first precession coil of length, l , and magnetic field, \mathbf{B} , along the neutron beam. The neutron spin thus undergoes a Larmor precession such that the total precession angle, φ , is given by the

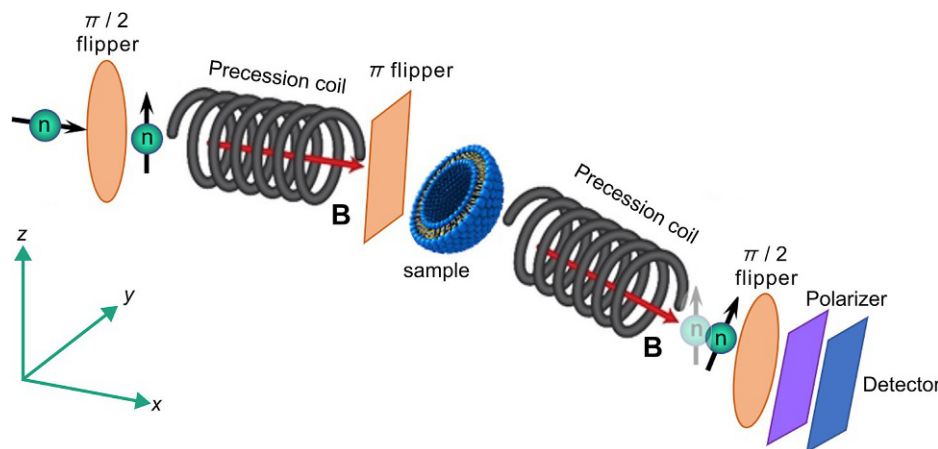


FIG. 3 Schematic diagram of a neutron spin echo (NSE) spectrometer. The magnetic elements of an NSE instrument are designed to manipulate the neutron spin (n) which encodes information about sample dynamics. The highlighted neutron indicates polarization loss (or change in spin orientation) due to energy exchange with the sample. In contrast, the transparent neutron represents a case with no energy exchange, resulting in an “echo” of the initial spin state. Adapted from Kumarage, T., Nguyen, J., & Ashkar, R. (2021). Neutron spin echo spectroscopy: A unique probe for lipid membrane dynamics and membrane-protein interactions. *Journal of Visualized Experiments*, 171, e62396.

magnetic field integral, $J = \int_0^l |\mathbf{B}| dx$, where $|\mathbf{B}| = B$ is the modulus of the magnetic induction. In other words, the precession angle is given by:

$$\varphi = \frac{\gamma \lambda m_n}{h} \int_0^l B dx \quad (5)$$

where $\gamma \approx -1.83 \times 10^8 \text{ rad s}^{-1} \text{ T}^{-1}$ is the magnetogyric ratio of the neutrons and $v_n = h/\lambda m_n$ is the neutron velocity, with m_n denoting the mass of the neutron, h the Planck constant, and λ the neutron wavelength. The change in polarization at the sample position is directly related to the normalized intermediate scattering function, $S(\mathbf{Q}, t)$, expressed as a function of Fourier time $t = \gamma B \hbar / m_n v_n^3$ (Ashkar, 2020; Mezei, 1972; Ohl et al., 2012).

Neutron spin echo spectrometers around the world are located at research reactors and pulsed neutron sources, e.g., BL-15 SNS-NSE at Oak Ridge National Laboratory (Ohl et al., 2012), CHRNS-NSE at the NIST Center for Neutron Research (Rosov, Rathgeber, & Monkenbusch, 1999), J-NSE at Heinz Maier-Leibnitz Zentrum (Holderer & Ivanova, 2015), and IN-11 and IN-15 at Institute Laue-Langevin (Farago, 1999). Most NSE spectrometers operate with energy resolutions, $\Delta \hbar \omega$, on the order of 10 neV (~ 100 ns), over length scales on the order of 1 to 250 Å (Monkenbusch & Richter, 2007; Monkenbusch, Schätzler, & Richter, 1997). In the previous expression, \hbar is the reduced Planck constant and ω is the neutron frequency. Notably, recent advances in the IN-15 NSE spectrometer at Institute Laue-Langevin have achieved energy resolutions as high as $\Delta \hbar \omega = 0.7 \text{ neV}$, yielding a maximum Fourier time, $t_{\text{max}} = 1 \mu\text{s}$ (Farago et al., 2015). These developments open new possibilities in exploring the dynamical hierarchy in membranes over extended timescales corresponding to vital membrane processes.

Membrane undulations

The stability and shape of membranes, and how they interact with cholesterol, proteins, or other foreign particles, such as drug molecules, depends on membrane undulations. These undulations are governed by membrane elastic properties, primarily the bending rigidity modulus, κ . Early NSE measurements provided direct experimental evidence that membrane bending undulations follow the elastic sheet model (Yamada et al., 2005). As predicted by Zilman and Granek (ZG), the signatures of such undulatory motions are manifested in relaxation spectra with stretched exponential decays given by (Zilman & Granek, 1996):

$$S_{ZG}(Q,t) = A \exp\left[-(\Gamma_{ZG}t)^{2/3}\right] \quad (6)$$

Here, A is the amplitude of the fluctuations and the parameter Γ_{ZG} is a Q -dependent decay rate which is directly related to the bending rigidity modulus. Indeed, stretched exponential decays of this form are typically observed in NSE relaxation spectra of vesicular membranes (Fig. 4A). The extraction of the bending rigidity modulus in these measurements entails refinements of the ZG theory (Watson & Brown, 2010) which take into account interleaflet friction to interpret the bending relaxation rate in terms of the effective bending modulus, κ . In this notation, κ is related to the bilayer bending modulus, κ , by $\kappa = \kappa + 2d^2k_m$, (Watson & Brown, 2010) where k_m is the monolayer area compressibility and d is the distance between the neutral surface and the bilayer midplane.

Considering the neutral surface (where the cross-sectional area per lipid molecule remains constant) to be at the interface between the hydrophilic head group and the hydrophobic fatty acid chains, the ZG relaxation rate for bending fluctuations can be expressed as (Hoffmann et al., 2014; Nagao et al., 2017):

$$\frac{\Gamma}{Q^3} = \frac{\Gamma_{ZG}}{Q^3} = 0.0069 \frac{k_B T}{\eta_s} \sqrt{\frac{k_B T}{\kappa}} \quad (7)$$

where η_s is the solvent viscosity, k_B is the Boltzmann constant, and T is the temperature on an absolute scale. A demonstration of the Q^3 -dependence of Γ_{ZG} is shown in Fig. 4B. Using this approach, the bending rigidity moduli κ have been reported for various phospholipid membranes in liquid-disordered and liquid-ordered states, yielding a direct measurement of membrane mechanics on nanoscopic scales (Arriaga et al., 2009; De Mel et al., 2020, 2021; Gupta et al., 2019; Gupta & Schneider, 2020; Lee et al., 2010; Sharma, Mamontov, Ohl, & Tyagi, 2017; Woodka et al., 2012). Although lipid membranes above their gel transition temperature are anticipated to have $\kappa \approx 20 k_B T$, a recent study (Gupta et al., 2018) showed that the membrane κ values strongly depended on the choice of solvent viscosity in Eq. (7), and deviated with increased viscosity of the suspending medium. Another study (Nagao et al., 2017) showed that while the bending rigidity of phospholipid membranes approached $20 k_B T$ well above their transition temperature, the bending rigidity exhibited a linear increase with temperature on approaching the gel transition. These observations are consistent with the temperature-dependent structural changes in the membrane measured by small-angle neutron scattering (SANS) and small-angle X-ray scattering (SAXS) (Kučerka, Nieh, & Katsaras, 2011), where the increase in temperature was found to linearly correlate with an increase in the area per lipid. Put together, these observations indicate that the decrease in molecular packing

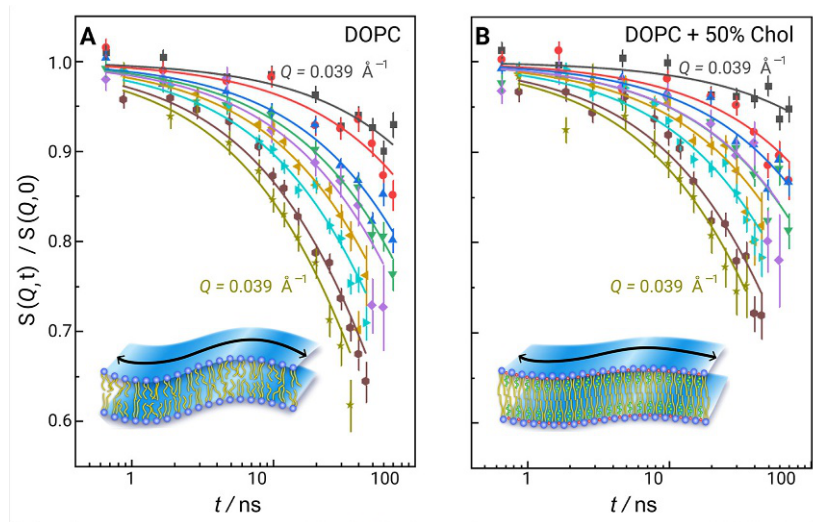


FIG. 4 Exponential decays observed in neutron spin echo (NSE) relaxation spectra of vesicular membranes capture membrane dynamics. (A) Normalized intermediate scattering functions, $S(Q,t)/S(Q,0)$, of DOPC liposomal membranes with 0 and 50 mol% cholesterol, along with stretched exponential fits (solid lines) given by Eq. (6). (B) The suppressed decays in DOPC/cholesterol membranes indicate slowdown in the measured dynamics. Adapted from Chakraborty, S., Doktorova, M., Molugu, T. R., Heberle, F. A., Scott, H. L., Dzikovski, B., et al. (2020). How cholesterol stiffens unsaturated lipid membranes. *Proceedings of the National Academy of Sciences of the United States of America*, 117, 21896–21905.

with temperature also affects the membrane elastic properties. Such a structure–property dependence was further verified by recent NSE experiments on binary lipid membranes demonstrating that elastic membrane properties, including the membrane bending rigidity and the area compressibility moduli, scale with the area per lipid (Kelley, Butler, Ashkar, Bradbury, & Nagao, 2020).

Similar observations were reported in another recent study by Chakraborty et al. investigating the effect of cholesterol on unsaturated DOPC lipid membranes (Chakraborty et al., 2020). Structurally, it is well known that cholesterol increases the molecular packing and thickness in DOPC bilayers, but, previous studies on DOPC/cholesterol membranes reported a lack of change in membrane rigidity even at cholesterol concentrations of up to 50 mol% (Gracià et al., 2010; Pan, Mills, Tristram-Nagle, & Nagle, 2008). In contrast, we (Chakraborty et al., 2020) showed that, on the length and time scales of NSE, cholesterol stiffened DOPC membranes in a way that was consistent with its effect on molecular packing. Fig. 4 shows the normalized intermediate scattering functions, $S(Q,t)/S(Q,0)$, measured by NSE on DOPC liposomes with 0 and 50 mol% cholesterol. The solid lines are fits of the data to the expression given by Eq. (6). The Q -dependence of the decay rates is illustrated in Fig. 5A, showing the classic Q^3 signature of bending fluctuations. In this illustration, the slope for Γ vs Q^3 is $\propto \sqrt{1/\kappa}$, hence the shallower slope observed for cholesterol-containing DOPC membranes indicates an increase in κ with increasing cholesterol content. To emphasize the structural dependence of the measured bending rigidity moduli, we (Chakraborty et al., 2020) showed that the bending rigidity modulus scales with the area per lipid, such that an increase in molecular packing with increasing cholesterol mole fraction directly correlates to an increase in the bending rigidity modulus

measured by NSE spectroscopy (Fig. 5B). Notably, the same conclusions were obtained by solid-state deuterium NMR relaxometry (Molugu & Brown, 2016) and real-space fluctuation analysis of MD simulations (Doktorova, Harries, & Khelashvili, 2017; Johner, Harries, & Khelashvili, 2016b) (see section “Membrane stiffening effect of cholesterol from molecular dynamics simulations”), confirming that similar observations persisted across these different approaches interrogating the membrane dynamics over analogous scales.

Furthermore, we point that analogous observations have been reported in NSE studies of monounsaturated POPC lipid membranes mixed with cholesterol (Arriaga et al., 2009, 2010). The study combined NSE and dynamic light scattering on large unilamellar vesicles to measure the bending rigidity constant and intermonolayer friction as a function of cholesterol content. The experiments concluded that the stiffening of POPC membranes by cholesterol was compatible with the structural condensation caused by hydrogen-bonding complexes between POPC and cholesterol (Arriaga et al., 2010), in line with the structure–property relations for DOPC bilayers discussed above.

Membrane thickness fluctuations

In addition to bending fluctuations, NSE can access another collective membrane fluctuation mode, namely membrane thickness fluctuations, by applying selective lipid deuteration. The hypothesis of thickness fluctuations, or breathing modes, in lipid membranes dates back to the early 1980s (Bach & Miller, 1980; Hladky & Gruen, 1982; Israelachvili & Wennerström, 1992; Miller, 1984). Biologically, this dynamic mode is associated with vital membrane processes including pore formation (Bennett, Sapay, & Tieleman, 2014; Movileanu, Popescu, Ion, & Popescu, 2006) and passive membrane permeation (Orsia & Essex, 2010). The first direct realization of thickness fluctuations in membranes was obtained using NSE experiments on

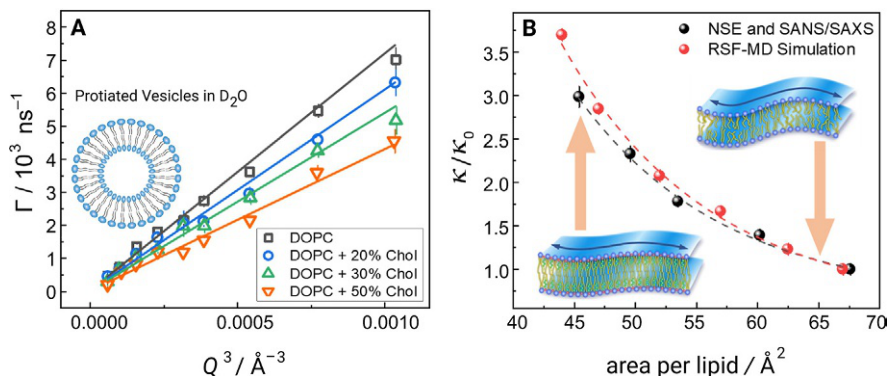


FIG. 5 Increase of bending rigidity modulus directly relates to increase in molecular packing with greater cholesterol mole fraction. (A) The Q -dependence of the decay rates $\Gamma(Q)$ follows the classic Q^3 behavior of bending undulations. (B) Fits of the decay rates to Eq. (7) yield the bending rigidity moduli, κ . The plots of κ vs. area per lipid indicate structural dependence of membrane mechanics on the molecular packing state obtained from SANS/SAXS studies. The results are confirmed by real-space fluctuation (RSF) analysis of atomistic molecular dynamics (MD) simulations. Adapted from Chakraborty, S., Doktorova, M., Molugu, T. R., Heberle, F. A., Scott, H. L., Dzиковski, B., et al. (2020). How cholesterol stiffens unsaturated lipid membranes. *Proceedings of the National Academy of Sciences of the United States of America*, 117, 21896–21905.

liposomal membranes prepared with chain-deuterated phospholipids (Woodka et al., 2012). These studies were partially enabled by the commensurate length scales (i.e., on the order of the membrane thickness) and timescales (~ 1 – 100 ns) accessible by NSE and partially by the inherent isotope sensitivity of neutrons. When chain deuterated variants of the lipids are used for the preparation of lipid vesicles in a deuterated solvent, the difference in the neutron contrast between the protiated lipid headgroups and the deuterated hydrocarbon chains amplifies the signal from changes in the membrane thickness, allowing selective measurements of the long-proposed thickness fluctuation mode. A similar deuteration scheme was used by Chakraborty et al. on cholesterol-containing di-monounsaturated DOPC lipid membranes (Chakraborty et al., 2020). The chain contrast-matched liposomes were prepared by using chain-perdeuterated DOPC- d_{66} and Chol- d_{40} , the former chemically synthesized using deuterated oleic acid and the latter obtained from genetically modified bacteria. The corresponding SANS data are illustrated in Fig. 6A, where the SANS scattering intensity is plotted as a function of the momentum transfer vector, Q . Here the lipid chains are contrast-matched with the solvent ($^2\text{H}_2\text{O}$) as schematically illustrated in Fig. 6B. It shows the effect of membrane thickening with increasing cholesterol content, indicated by decreasing Q -values of the scattering intensity minimum (shaded arrow).

In this type of contrast-variation experiment, the enhanced dynamics beyond bending fluctuations are most pronounced at Q -values that correspond to the membrane thickness (Fig. 6B). This observation has been recently corroborated by ultra-coarse-grained MD simulations (Carrillo, Katsaras, Sumpter, & Ashkar, 2017) on real-size liposomes. The thickness fluctuation signals are schematically illustrated in Fig. 6C right-bottom corner. The data for membrane fluctuations are modeled following the formalism developed by Nagao et al. (2017), which connects the amplitude and rate of the fluctuations to biophysical membrane parameters, including the membrane viscosity and area compressibility modulus. This

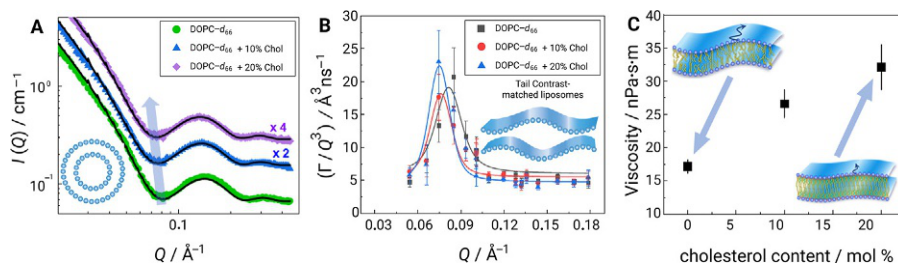


FIG. 6 Small-angle neutron scattering data from selectively deuterated liposomes. (A) Data for vesicles of chain-perdeuterated DOPC/cholesterol membranes show thickening with greater cholesterol content, indicated by decreasing Q values of the SANS scattering intensity minimum. The data are vertically scaled for proper visualization. The solid lines are fits using a core multishell model. Inset: geometrical illustrations of chain contrast-matched liposomes. (B) The NSE relaxation rates measured using deuterated DOPC/cholesterol membranes in deuterated buffer solution. These fluctuations are manifested as additional dynamics superimposed on the Q^3 signal arising from bending relaxation. (C) Fits of the thickness fluctuation signals using Eq. (8) show greater membrane viscosity with increasing mol% cholesterol. Adapted from Chakraborty, S., Doktorova, M., Molugu, T. R., Heberle, F. A., Scott, H. L., Dzikowski, B., et al. (2020). How cholesterol stiffens unsaturated lipid membranes. *Proceedings of the National Academy of Sciences of the United States of America*, 117, 21896–21905.

treatment extrapolates the theoretical framework by [Bingham, Smye, and Olmsted \(2015\)](#). In this approach, the thickness fluctuation signal is given by:

$$\frac{\Gamma}{Q^3} = \frac{\Gamma_{ZC}}{Q^3} = \frac{K_A k_B T}{\mu Q_0^3 k_B T + 4\mu Q_0 K_A A_0 (Q - Q_0)^2} \quad (8)$$

where Q_0 is the peak Q -value obtained from SANS, μ is the internal membrane bilayer viscosity, and K_A is the area compressibility modulus obtained from NSE bending rigidity measurements. Notice that the membrane viscosity, μ , is the only fitting parameter in Eq. (8). In our study ([Chakraborty et al., 2020](#)), we used this approach to inspect the effect of cholesterol on membrane viscosity. Our measurements were performed on DOPC- d_{66} membranes with 0, 10, and 20 mol% of Chol- d_{40} ([Chakraborty et al., 2020](#)), and showed that the membrane viscosity increases with increased cholesterol content (Fig. 6C).

However, we point out that expressing the membrane viscoelastic behavior using Eq. (8) requires an understanding of the connection between area compressibility and bending rigidity. Based on models for elastic thin-sheet deformation ([Rawicz, Olbrich, McIntosh, Needham, & Evans, 2000](#)), the bending rigidity modulus, κ , is proportional to the area compressibility modulus, K_A , according to: $\kappa = K_A t_m^2 / \zeta$, where t_m is the mechanical (or deformable) membrane thickness, and ζ is a constant describing the interleaflet coupling. According to the polymer brush model, $\zeta = 24$ for lightly coupled leaflets, typical of fluid lipid membranes ([Rawicz et al., 2000](#)). By contrast, [Pan et al. \(2009\)](#) have suggested that the polymer brush model does not hold for cholesterol-containing unsaturated lipid membranes. Nonetheless [Doktorova, LeVine, et al. \(2019\)](#), using MD simulations and a modified assignment of the mechanical membrane thickness, have concluded that the polymer brush model indeed holds for a wide range of membrane types, including unsaturated lipid membranes containing cholesterol. Employing the modified polymer brush model, [Chakraborty et al. \(2020\)](#) compared the membrane rigidity from fully protiated DOPC and area compressibility modulus from chain contrast-matched lipids and found consistent effects of cholesterol on membrane viscosity, i.e., the increase in cholesterol content resulted in greater membrane viscosity. Next, we discuss how solid-state ^2H NMR measurements yield a similar increase in the bending modulus, as observed by NSE, confirming the membrane stiffening effect of cholesterol over comparable length and time scales.

Solid-state ^2H NMR spectroscopy of lipid membranes

Solid-state nuclear magnetic resonance (NMR) spectroscopy is an atomic-level method to determine the structure and dynamics of solids and semi-solids ([Reif, Ashbrook, Emsley, & Hong, 2021](#)) and is highly complementary to NSE methods. In particular, solid-state ^2H NMR spectroscopy has long been regarded as one of the premier biophysical techniques applicable to lipid bilayers and biomembranes ([Brown & Chan, 1996](#)). It is a versatile method for studying the molecular organization of lipids within membranes, including the structure, ordering, and rates of molecular motions. Solid-state NMR investigates the biophysical properties of lipid membranes and provides information complementary to other spectroscopic techniques. By combining solid-state ^2H NMR order parameter measurements with nuclear spin relaxation experiments, one can obtain atomistically resolved information about collective

membrane dynamics, such as elastic deformations of the acyl chain region within the membrane. The NMR technology provides insights on membrane properties that cannot be obtained with other existing methods. Because of their physiological liquid-crystalline nature, membrane elastic deformations together with their multiscale molecular dynamics clearly fall in the solid-state ^2H NMR time and length scales, which allow for a detailed analysis of membrane fluctuations in the presence of cholesterol.

Introducing site-specific ^2H labels, due to the individual C– ^2H bonds, allows atomic-level details for noncrystalline amorphous or liquid-crystalline systems to be obtained. As the coupling interactions in solid-state NMR are sensitive to orientation and/or distance, their values correspond with the average structure of the system under study. The relaxation parameters derived from solid-state ^2H NMR spectroscopy give additional insight into the relevant molecular motions. One of the distinctive characteristics in solid-state ^2H NMR of biomolecular systems is that both lineshape data (Molugu, Lee, & Brown, 2017) and relaxation times (Martinez, Dykstra, Lope-Piedrafita, Job, & Brown, 2002) are accessible. An example for investigating structural dynamics using ^2H NMR is shown in Fig. 7. The information obtained involves the molecular motions, including a range of timescales. The combined measurements of residual quadrupolar couplings (RQCs) and relaxation rates provide information on the geometry and allow investigations of multiscale molecular motions and their amplitudes in the membrane systems of interest.

Solid-state ^2H NMR spectroscopic principles

Before we move on to the applications, knowing the basics of ^2H NMR spectroscopy will be useful in understanding the information that is derived. We know that the ^2H nucleus has a spin of $I=1$, and hence there are three Zeeman energy levels due to projecting the nuclear

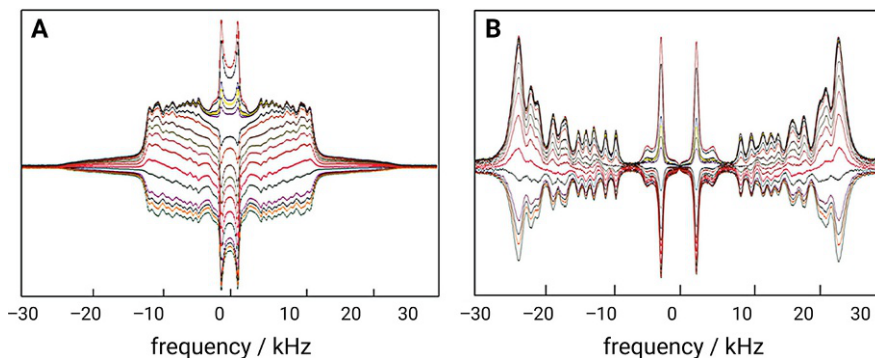


FIG. 7 Solid-state ^2H NMR spectroscopy of membrane lipids provides both lineshape data and relaxation times. (A) Experimental ^2H NMR spectra, and (B) numerically inverted (de-Paked) ^2H NMR spectra ($\theta=0^\circ$) as a function of the variable delay between the inversion pulse and spectral acquisition for DMPC- d_{54} in the liquid-disordered (l_d) phase. The de-Paked spectra show a high degree of packing at the level of phospholipid headgroups of both leaflets of the bilayer along with high density of the bilayer core at the leaflet interface. They correspond to single bilayer orientation and are more highly resolved, enabling accurate determination of the spectral parameters. Data were obtained at 76.8 MHz (magnetic field strength of 11.7 T) using an inversion-recovery pulse sequence, $(\pi)x-t_1-(\pi/2)x-\tau_1-(\pi/2)_y-\tau_2$ -acquire, with the variable delay t_1 ranging from 5 ms to 3 s. Adapted from Martinez, G. V., Dykstra, E. M., Lope-Piedrafita, S., Job, C., & Brown, M. F. (2002). NMR elastometry of fluid membranes in the mesoscopic regime. *Physical Review E*, 66, 050902–050906, with permission of American Physical Society.

spin angular momentum onto the magnetic field direction. The three eigenstates $|m\rangle = |0\rangle$ and $|\pm 1\rangle$ are given by the Hamiltonian \hat{H}_z for interaction of the nuclear magnetic moment with the static magnetic field. Because shifts between adjacent spin energy levels are allowed, this will yield two single-quantum nuclear spin transitions. Moreover, due to the quadrupolar coupling the degeneracy of the allowed transitions in ^2H NMR is removed. The perturbing Hamiltonian \hat{H}_Q comes from the interaction of the quadrupole moment of the ^2H nucleus with the electric field gradient (EFG) of the $\text{C}-^2\text{H}$ bond. Hence, for each inequivalent site, two spectral branches are obtained in the experimental spectrum.

In solid-state ^2H NMR spectroscopy, the experimentally observed quadrupolar coupling is given by the difference in the frequencies $\Delta\nu_Q^\pm = \Delta\nu_Q^+ - \Delta\nu_Q^-$ of the spectral lines due to the perturbing Hamiltonian. The result for the quadrupolar frequencies (ν_Q^\pm) is given by:

$$\nu_Q^\pm = \pm \frac{3}{4} \chi_Q \left\{ D_{00}^{(2)}(\Omega_{\text{PL}}) - \frac{\eta_Q}{\sqrt{6}} \left[D_{-20}^{(2)}(\Omega_{\text{PL}}) + D_{20}^{(2)}(\Omega_{\text{PL}}) \right] \right\} \quad (9)$$

Here, $\chi_Q \equiv e^2qQ/h$ is the *static* quadrupolar coupling constant, η_Q corresponds to the asymmetry parameter of the EFG tensor, $D_{m0}^{(2)}(\Omega_{\text{PL}})$ is a Wigner rotation matrix element, where $m = 0, \pm 1, \pm 2$ and $\Omega_{\text{PL}} \equiv (\alpha_{\text{PL}}, \beta_{\text{PL}}, \gamma_{\text{PL}})$ are the Euler angles (Molugu et al., 2017; Rose, 1957) relating the principal axis system (PAS) of the EFG tensor (P) to the laboratory frame (L) (Brown, 1996; Leftin, Xu, & Brown, 2014; Xu, Struts, & Brown, 2014). Because the static EFG tensor of the $\text{C}-^2\text{H}$ bond is nearly axially symmetric ($\eta_Q \approx 0$), the above result simplifies to:

$$\nu_Q^\pm = \pm \frac{3}{4} \chi_Q D_{00}^{(2)}(\Omega_{\text{PL}}) \quad (10)$$

The experimental quadrupolar splitting is thus obtained as:

$$\Delta\nu_Q = \frac{3}{2} \chi_Q D_{00}^{(2)}(\Omega_{\text{PL}}) \quad (11)$$

where the various symbols are defined above. In liquid-crystalline membranes, the molecular motions are often cylindrically symmetric about the bilayer normal, an axis known as the director. Rotation of the principal axis system of the coupling tensor to the laboratory frame, described by the three Ω_{PL} Euler angles (see above), can thus be represented by two consecutive rotations. First, the Euler angles $\Omega_{\text{PD}}(t)$ represent the (time-dependent) rotation from the principal axis frame to the director frame, and second the Euler angles Ω_{DL} represent the (static) rotation from the director frame to laboratory frame. Use of the closure property of the rotation group (Xu et al., 2014) is helpful in this regard. Considering the cylindrical symmetry about the director, we can then expand Eq. (11), which now reads:

$$\Delta\nu_Q = \frac{3}{2} \chi_Q \langle D_{00}^{(2)}(\Omega_{\text{PD}}) \rangle D_{00}^{(2)}(\Omega_{\text{DL}}) \quad (12a)$$

$$= \frac{3}{2} \chi_Q \frac{1}{2} \langle 3 \cos^2 \beta_{\text{PD}} - 1 \rangle \frac{1}{2} (3 \cos^2 \beta_{\text{DL}} - 1) \quad (12b)$$

Here, $\beta_{\text{DL}} \equiv \theta$ is the angle the bilayer normal makes to the static external magnetic field. The segmental order parameter S_{CD} is given by:

$$S_{\text{CD}} = \frac{1}{2} \langle 3 \cos^2 \beta_{\text{PD}} - 1 \rangle \quad (13)$$

where the angular brackets denote a time or ensemble average. It follows that

$$\Delta v_{\text{Q}} = \frac{3}{2} \chi_{\text{Q}} S_{\text{CD}} P_2(\cos \beta_{\text{DL}}) \quad (14)$$

in which $P_2(\cos \beta_{\text{DL}}) \equiv (3 \cos^2 \beta_{\text{DL}} - 1)/2$ is the second-order Legendre polynomial. The above formula shows the dependence of the quadrupolar splitting on the (Euler) angles that rotate the coupling tensor from its principal axes system to the laboratory frame of the main magnetic field (Molugu et al., 2017).

The process of NMR relaxation comes from fluctuations of the coupling Hamiltonian due to the various motions of the lipid molecules within the bilayer. These fluctuations give rise to transitions between the different adjacent energy levels (Xu et al., 2014). In solid-state ^2H NMR relaxometry of liquid-crystalline membrane lipids, we are often interested in the spin-lattice (R_{1Z}) relaxation rates. Experimental measurements of the R_{1Z} relaxation rate involve inverting (flipping) the magnetization, and then following the attainment of equilibrium by the magnetization recovery as a function of time. The observable relaxation rates are related to the spectral densities of motion in the laboratory frame by:

$$R_{1Z} = \frac{3}{4} \pi^2 \chi_{\text{Q}}^2 [J_1(\omega_0) + 4J_2(2\omega_0)] \quad (15)$$

In this formula, R_{1Z} is the spin-lattice (longitudinal) relaxation rate, and $J_m(m\omega_0)$ denotes the spectral densities of motion, where $m=1, 2$, and ω_0 is the deuteron Larmor frequency. The spectral densities $J_m(m\omega_0)$ describe the power spectrum of the motions as a function of frequency ω_0 in terms of fluctuations of the Wigner rotation matrix elements for transforming the coupling (EFG) tensor from its principal axis system to the laboratory frame. They are the Fourier transform partners of the orientational correlation functions $G_m(t)$, which depend on time and thereby characterize the C^{-2}H bond fluctuations of the lipids.

Clearly, the segmental order parameters (Fig. 8A) depend only on the amplitudes of the C^{-2}H bond motions, while the relaxation rates (Fig. 8B) also depend on the rates of the C^{-2}H bond fluctuations. According to a generalized model-free (GMF) approach of relaxation rate analysis (Brown, 1984; Xu et al., 2014), a simple dependence of the R_{1Z} rates on the squared segmental order parameters (S_{CD}^2) (square-law) along the chain would result (Fig. 8C). For short-wavelength excitations, on the order of the bilayer thickness and less, the spectral density is written as (Nevzorov & Brown, 1997):

$$J_m(\omega) = \frac{5}{2} S_{\text{CD}}^2 D \omega^{-(2-d/2)} \left[\left| D_{-1m}^{(2)}(\beta_{\text{DL}}) \right|^2 + \left| D_{1m}^{(2)}(\beta_{\text{DL}}) \right|^2 \right] \quad (16)$$

Here, ω is the angular frequency, D is the viscoelastic constant, d is the dimensionality, and $D^{(2)}$ indicates the second-rank Wigner rotation matrix (Rose, 1957). The spectral densities $J_m(\omega)$ depend on the square of the observed S_{CD} order parameters, and the slope of the square-law plot is inversely related to the softness of the membrane. For 3D quasielastic fluctuations, the viscoelastic constant is given by: $D = 3k_{\text{B}}T\sqrt{\eta} / 5\pi\sqrt{2}K^3S_{\text{s}}^2$, where a single elastic constant K is assumed, in which η is the corresponding viscosity coefficient, S_{s} is the order

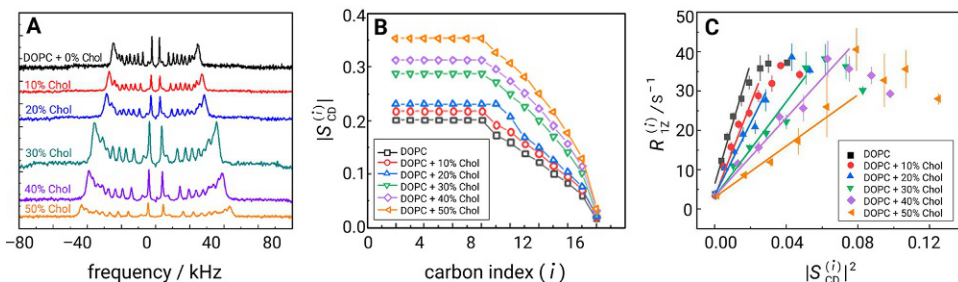


FIG. 8 Cholesterol increases acyl chain ordering in unsaturated DOPC lipid membranes. (A) De-Paked solid-state ^2H NMR spectra of DOPC/cholesterol membranes show greater quadrupolar splittings with increasing cholesterol fraction. (B) Segmental order parameter versus acyl position for POPC- d_{31} probe lipid in DOPC/cholesterol membranes with different mol% cholesterol at $T=25^\circ\text{C}$. (C) Dependence of spin-lattice relaxation rate $R_{1Z}^{(i)}$ on squared order parameters $S_{CD}^{(i)}$ indicating a decrease in square-law slopes due to bilayer stiffening by cholesterol. Adapted from Chakraborty, S., Doktorova, M., Molugu, T. R., Heberle, F. A., Scott, H. L., Dzikovski, B., et al. (2020). How cholesterol stiffens unsaturated lipid membranes. *Proceedings of the National Academy of Sciences of the United States of America*, 117, 21896–21905.

parameter for the relatively slow motions, and other symbols have their usual meanings. A single elastic constant is assumed, and no distinction is made between splay, twist, and bend deformations. In addition to the bending modulus κ , the compression modulus K_B comes into play (Nagle & Tristram-Nagle, 2000). For splay deformations, the bending rigidity is: $\kappa \approx Kt$, where $t=2D_C$ is the bilayer thickness, giving a $\kappa^{-3/2}$ dependence of the R_{1Z} rates (Brown, Thurmond, Dodd, Otten, & Beyer, 2001).

Membrane dynamics and structural properties by solid-state ^2H NMR spectroscopy

In general, the deformation of a membrane bilayer can be characterized by four constants: (i) the surface tension (which is zero for a bilayer at equilibrium), (ii) the area expansion modulus or alternatively the compressibility modulus, (iii) the bending rigidity κ , and (iv) the monolayer spontaneous curvature. These structural quantities are fundamental to the forces governing the nanoscopic structures of the lipid membrane assemblies. Representative applications of solid-state ^2H NMR spectroscopy to lipid membranes include the influence of cholesterol (Brown et al., 2001; Brown & Seelig, 1978; Trouard et al., 1999) as well as acyl chain unsaturation. Here we are interested in the average membrane structure, fluctuations, and elastic deformations due to the cholesterol. As a steroid molecule, cholesterol is amphiphilic in nature as in the case of other lipids (Fig. 2B–E). Our emphasis is on the membrane structural deformation and emergent fluctuations at an atomistic level. For acyl chain perdeuterated phospholipids, we deconvolute or de-Pake the powder-type spectra of random multilamellar dispersions to obtain more highly resolved subspectra corresponding to the $\theta=0^\circ$ orientation (Fig. 8A). The resolved signals show a progressive increase in the splittings with increasing mole fraction of cholesterol (Fig. 8A). Interaction with the rigid cholesterol molecule leads to a substantial reduction of the number of degrees of freedom of the flexible phospholipids, as evidenced by the larger residual quadrupolar splittings.

According to Eq. (14) the observed residual quadrupolar coupling $\Delta\nu_Q$ is directly related to the segmental order parameter S_{CD} . The residual quadrupolar couplings vary substantially, giving a profile of the absolute segmental order parameter $S_{\text{CD}}^{(i)}$ as a function of chain position (index i). This inequivalence comes from the effects of the bilayer packing on the *trans-gauche* isomerizations of the acyl groups. Fig. 8B shows the segmental order parameters $S_{\text{CD}}^{(i)}$ plotted as a function of the acyl position (index i) for DOPC alone and DOPC in the presence of cholesterol. The plateau region in the order profiles (Fig. 8B) can be explained by the preferred configurations of the acyl chains parallel to the membrane normal. Thus, the smaller absolute $S_{\text{CD}}^{(i)}$ values for DOPC in the absence of cholesterol manifest the additional degrees of freedom of the unsaturated acyl chains.

Clearly, the segmental order parameters depend on the amplitudes of the C– ^2H bond fluctuations while the relaxation rates depend on both the angular amplitudes and the rates of the C– ^2H bond motions. Hence the ordering and rate of motion must be distinguished in explaining the relaxation of lipid bilayers (Brown, 1979). In ^2H NMR spectroscopy of membranes, the measurements comprise the order parameter and the relaxation rate profiles (Fig. 8). This dependence on the motional amplitudes gives a signature of relatively slow bilayer motions that modulate the residual coupling tensors left over from local segmental motions (Fig. 8C). Provided a simple composite membrane deformation model applies (Brown, Thurmond, Dodd, Otten, & Beyer, 2002; Nevzorov, Trouard, & Brown, 1998), the R_{1Z} rates manifest a broad spectrum of 3D collective bilayer excitations together with effective rotations of the lipids. Transverse ^2H NMR spin relaxation studies likewise provide evidence for 2D collective motions of the membrane film at lower frequencies (Althoff, Frezzato, et al., 2002; Althoff, Stauch, et al., 2002; Bloom & Evans, 1991; Bloom, Evans, & Mouritsen, 1991; Molugu, Mallikarjunaiah, Job, & Brown, 2012, 2013).

Solid-state ^2H NMR studies clearly show the influence of cholesterol on the physical properties of 1,2-diperdeuteriomyristoyl-*sn*-glycero-3-phosphocholine (DMPC- d_{54}) bilayers at an atomistic level (Fig. 9A–D). A gradual increase in the quadrupolar splittings ($\Delta\nu_Q$) for the acyl segments is observed as cholesterol concentration is increased, which reflects larger orientational order of the acyl chain segments versus the bilayer normal. This finding explains the well-known condensing effect of cholesterol at the molecular level, involving a decrease of the area per phospholipid molecule at the aqueous interface, accompanied by greater bilayer hydrocarbon thickness. The experimental solid-state ^2H NMR relaxation studies of the effect of cholesterol on lipid bilayers further show a square-law functional dependence of the R_{1Z} rates versus the order parameters S_{CD} along the entire acyl chain for the multilamellar dispersions of DMPC- d_{54} /cholesterol bilayers (Fig. 9E). Notice that the square-law functional dependence (Brown, 1982) is a model-free correlation among the experimental observables (Fig. 8C and Fig. 9E). Here the progressive increase in the bilayer rigidity of DMPC lipid bilayers obtained by solid-state ^2H NMR relaxation at various compositions of DMPC and cholesterol is manifested by the square-law slope. Cholesterol yields a large decrease in the square-law slopes, corresponding to a progressive reduction in bilayer elasticity (Figs. 8C and 9E). By contrast, local *trans-gauche* isomerizations along the chain do not yield such a square-law as indicated for DOPC/cholesterol membranes. The reduction in the square-law slope (Fig. 9E) reflects an increase in bending rigidity κ due to short-range cholesterol–phospholipid interactions, showing how membrane mechanical properties emerge for the local atomistic forces within the lipid bilayer.

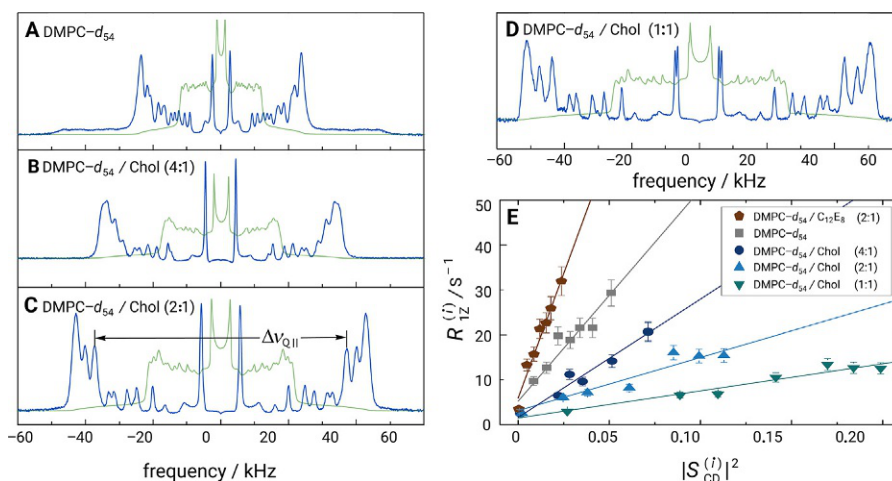


FIG. 9 Cholesterol reduces the conformational degrees of freedom for the acyl chain segment orientations. (A) DMPC-*d*₅₄ in the liquid-disordered (*l*_d) phase, and (B–D) DMPC-*d*₅₄ containing various mole fractions of cholesterol in the liquid-ordered (*l*_o) phase. Powder type spectra (green) of randomly oriented multilamellar dispersions were numerically inverted (de-Paked) to yield subspectra corresponding to the $\theta=0^\circ$ orientation (blue). Note that a distribution of residual quadrupolar couplings (RQCs) corresponds to the various C²H₂ and C²H₃ groups with a progressive increase due to cholesterol. (E) Dependence of spin-lattice relaxation rates $R_{12}^{(i)}$ on squared order parameters $S_{CD}^{(i)}$ for resolved ²H NMR splittings of DMPC-*d*₅₄. Data in A–E were obtained at $T=44^\circ\text{C}$ and at 76.8 MHz (11.8 T). Adapted from Martinez, G. V., Dykstra, E. M., Lope-Piedrafita, S., & Brown, M. F. (2004). Lanosterol and cholesterol-induced variations in bilayer elasticity probed by ²H NMR relaxation. *Langmuir*, 20, 1043–1046.

Membrane stiffening effect of cholesterol from molecular dynamics simulations

Experimental observations of membrane structure and dynamics are invariably limited in resolution, both spatial and temporal, depending on the biophysical method employed. Stemming from the rapid growth of computer power, molecular dynamics (MD) simulations are starting to play an increasingly prominent role in interpreting experimental results, further enabling understanding of lipid membranes. Because the length and time scales probed by MD simulations parallel those of experiments, the synergy between spectroscopic techniques and atomistic models offers new avenues to exploring membrane biophysics. Acyl chain order parameters measured with NMR have been historically used to validate simulation force fields (Vermeer, De Groot, Reat, Milon, & Czaplicki, 2007), while results from MD trajectories have provided details otherwise inaccessible by experiment (Ballweg et al., 2020; Doktorova, Heberle, et al., 2017, 2019). Analyses of local fluctuations in leaflet thickness (Doktorova, LeVine, et al., 2019) and lipid splay angles (i.e., the angle between pairs of lipid director vectors) (Doktorova, Harries, & Khelashvili, 2017; Johner et al., 2016b; Johner, Harries, & Khelashvili, 2016a) from MD trajectories have been shown to yield the area compressibility and bending moduli of a bilayer, providing new tools for examining cholesterol effects on membrane mechanical properties. The latter method relies on calculating the distribution

of splay angles of neighboring lipid molecules, converting it to a potential of mean force (PMF) (Doktorova, Harries, & Khelashvili, 2017; Johner et al., 2016a, 2016b; Johner, Harries, & Khelashvili, 2014), from which the bilayer bending modulus emerges. This method has been shown to provide reliable moduli for a large number of model membranes (Doktorova, Harries, & Khelashvili, 2017), including lipid mixtures and finite-size nanodisc membranes (Schachter, Allolio, Khelashvili, & Harries, 2020). It was recently applied in conjunction with our NSE and NMR measurements to probe the trends in bending rigidity of unsaturated DOPC membranes with increasing amounts of cholesterol (Chakraborty et al., 2020). The results from the simulations are in excellent agreement with experimental methods (see Fig. 5) and further reveal information about the length and time scale dependence of the bending moduli. The analysis shows that cholesterol increases the orientational order in the DOPC bilayers, i.e., the order parameter of the splay angle between lipid pairs as a function of distance between the lipids, in a concentration dependent manner. Even at the highest cholesterol concentration of 50 mol% the orientational order in the DOPC/cholesterol membrane is less than for a sphingomyelin (SM) bilayer with 30 mol% cholesterol. Similarly, the lipid splay angles are correlated over longer time scales in the SM/cholesterol bilayer relative to all the DOPC/cholesterol compositions. These results constitute the first steps towards our molecular understanding of the measured differences in bending moduli of lipid bilayers.

Cholesterol effects on drug uptake and drug delivery applications

Given the structural and mechanical effects of cholesterol on lipid membranes discussed above, one can expect the presence of cholesterol to impact the design, uptake, and delivery of cell-targeted drugs. This includes the propensity of drug molecules to incorporate into cholesterol-rich membranes, the resistance of membranes to lysis by drugs or pathogens, and the stability of synthetic membranes used in liposomal drug delivery applications. For example, solid-state ^2H NMR spectroscopy has been used for tracking and understanding the nature of lipid-cholesterol interactions with local anesthetics. Benzocaine, a local anesthetic, is known to reduce the ordering effect of cholesterol on the acyl chains of phospholipid membranes, which helps pinpoint the interaction site of neutral anesthetics in sodium channels of cellular membranes (Kuroda, Nasu, Fujiwara, & Nakagawa, 2000). Additional research has studied the interactions of the local anesthetic tetracaine under charged and uncharged pH conditions in multilamellar lipid dispersions with cholesterol (Auger et al., 1988). The higher partition coefficients obtained at alkaline pH are indicative of hydrophobic interactions of the uncharged anesthetic with the hydrocarbon region of the lipid bilayer. Locations of charged and uncharged tetracaine in cholesterol-containing systems are markedly different than pure PC bilayers (Auger et al., 1988). For bilayers containing cholesterol, the smaller partition coefficients at both acidic and alkaline pH values suggest the solubility of tetracaine is reduced by increasing the order of the lipid chains (recall that “like dissolves like”). Studies of benzyl alcohol have furthermore shown that at concentrations used for local anesthesia there is no change in membrane thickness. At higher concentrations, disordering of the lipid chains is found that is opposite to cholesterol (Turner & Oldfield, 1979), which could explain the cholesterol-induced reduction in anesthetic solubility. Biophysical influences of general anesthetics also depend on ordering of the acyl chains in the host phospholipid bilayer, as in the case of 1-octanol

or 1-decanol, which reduce the acyl chain order only slightly in the gel (solid-ordered) phase, yet substantially in the liquid-crystalline (liquid-disordered) phase (Thewalt & Cushley, 1987). Hence the disordering effects of anesthetics are dependent on the presence of cholesterol in the liquid-ordered state of the lipid dispersions (Thewalt & Cushley, 1987).

Numerous additional studies illustrate how cholesterol plays a pivotal role in drug delivery and pharmaceutical applications. These studies provide vital information about the stability of liposomes with membrane-incorporated drugs, and about variations in membrane elasticity in diseased cells. For example, cholesterol plays an important role in drug delivery applications involving antimicrobial peptides which are found in different life forms, including bacteria, plants, fish, and mammals, and act as therapeutic agents against a wide range of infections even in cancer cells (Brogden, 2005; Zasloff, 2002). Studies using solid-state ^2H NMR spectroscopy have shown that antimicrobial peptides tend to locate near the polar-apolar interface of the membrane (Sandhu, Booth, & Morrow, 2020; Sherman et al., 2009), causing a disruption in molecular packing. These observations are in alignment with neutron spin echo measurements revealing an overall decrease in membrane rigidity (Lee et al., 2010). Similarly, from solid-state ^2H NMR studies we know how charged peptides can interact and translocate through phospholipid bilayers into the cytosol to deliver biopharmaceuticals (Su, Li, & Hong, 2013). Notably the presence of cholesterol reduces the activity of antimicrobial peptides (Matsuzaki, 1999) and results in the protection of cells, such as human erythrocytes, from membrane-permeating peptides like magainin 2 (Matsuzaki, Sugishita, Fujii, & Miyajima, 1995). These studies highlight the importance of cholesterol in stabilizing the membranes of healthy cells in therapeutic applications utilizing antimicrobial peptides for attacking infectious cells. The membrane-stabilizing property of cholesterol also plays a protective role in therapeutic applications involving membrane disrupting drug molecules. For example, the nephrotoxicity of “last-line” antibiotics like polymyxin B has been investigated by a combination of X-ray diffraction and molecular dynamics (MD) simulations to track the membrane structural instabilities leading to water intake in the membrane core (Khondker et al., 2017). Cholesterol-rich membranes exhibit higher stability and reduced leakage, resulting in a considerable reduction in membrane damage in kidney cell membranes.

Conclusions

The cholesterol-induced variations in membrane dynamics from different studies pinpoint a general understanding of the underlying molecular interactions. The simultaneous increase in cholesterol-induced molecular packing, membrane viscosity, and bending rigidity (Chakraborty et al., 2020) indicates a molecular-level suppression of elastic fluctuations that alter the local viscoelastic properties of the membrane for both saturated and unsaturated bilayers. Similar results have been reported for unsaturated lipid membranes by neutron spin echo measurements (Arriaga et al., 2009, 2010), as in the case of solid-state ^2H NMR spectroscopy (Martinez et al., 2002; Molugu & Brown, 2016). Therefore, from the existing literature a clear correlation can be drawn in favor of an overall increase in membrane rigidity and molecular packing due to interactions with cholesterol. These findings have significant implications for the role of cholesterol in drug incorporation into cell membranes

and in the formulation of stable liposomes for leak-proof stable drug delivery. This aspect is crucial for the development of next-generation drugs and for studying their effects on live cell membranes with different cholesterol contents. The stiffening of membranes by cholesterol also impacts our understanding of viral infections, including the coronavirus SARS-CoV-2 pandemic. One expects that the fusion, maturation, and budding of viral particles closely depends on the mechanical properties of contact membrane sites, determined by their lipidic and cholesterol content.

Acknowledgment

R.A. was supported by faculty startup funds from the state of Virginia and NSF (MCB-2137154). M. D. was supported by an NIH Ruth L. Kirschstein Postdoctoral Individual National Research Service Award (1F32GM134704). G. K. is supported by an award from the 1923 Fund. M. F. B. gratefully acknowledges support from the NIH (R01EY026041) and NSF (MCB-1817862 and CHE-1904125).

References

- Allen, T. M., & Cullis, P. R. (2013). Liposomal drug delivery systems: From concept to clinical applications. *Advanced Drug Delivery Reviews*, *65*, 36–48.
- Althoff, G., Frezzato, D., Vilfan, M., Stauch, O., Schubert, R., Vilfan, I., et al. (2002). Transverse nuclear spin relaxation studies of viscoelastic properties of membrane vesicles. I. Theory. *The Journal of Physical Chemistry B*, *106*, 5506–5516.
- Althoff, G., Stauch, O., Vilfan, M., Frezzato, D., Moro, G. J., Hauser, P., et al. (2002). Transverse nuclear spin relaxation studies of viscoelastic properties of membrane vesicles. II. Experimental results. *The Journal of Physical Chemistry B*, *106*, 5517–5526.
- Arriaga, L. R., López-Montero, I., Orts-Gil, G., Farago, B., Hellweg, T., & Monroy, F. (2009). Fluctuation dynamics of spherical vesicles: Frustration of regular bulk dissipation into subdiffusive relaxation. *Physical Review E*, *80*, 031908.
- Arriaga, L. R., Rodríguez-García, R., López-Montero, I., Farago, B., Hellweg, T., & Monroy, F. (2010). Dissipative curvature fluctuations in bilayer vesicles: Coexistence of pure-bending and hybrid curvature-compression modes. *European Physical Journal E*, *31*, 105–113.
- Ashkar, R. (2020). Selective dynamics in polymeric materials: Insights from quasi-elastic neutron scattering spectroscopy. *Journal of Applied Physics*, *127*, 151101–151118.
- Ashkar, R., Bilheux, H. Z., Bordallo, H., Briber, R., Callaway, D. J. E., & Cheng, X. (2018). Neutron scattering in the biological sciences: Progress and prospects. *Acta Crystallographica D*, *74*, 1129–1168.
- Ashkar, R., Nagao, M., Butler, P. D., Woodka, A. C., Sen, M. K., & Koga, T. (2015). Tuning membrane thickness fluctuations in model lipid bilayers. *Biophysical Journal*, *109*, 106–112.
- Auger, M., Jarrell, H. C., & Smith, I. C. (1988). Interactions of the local anesthetic tetracaine with membranes containing phosphatidylcholine and cholesterol: A ^2H NMR study. *Biochemistry*, *27*, 4660–4667.
- Bach, D., & Miller, I. R. (1980). Glycerol monooleate black lipid membranes obtained from squalene solutions. *Biophysical Journal*, *29*, 183–187.
- Ballweg, S., Sezgin, E., Doktorova, M., Covino, R., Reinhard, J., Wunnicke, D., et al. (2020). Regulation of lipid saturation without sensing membrane fluidity. *Nature Communications*, *11*, 756.
- Bassereau, P., Sorre, B., & Lévy, A. (2014). Bending lipid membranes: Experiments after W. Helfrich's model. *Advances in Colloid and Interface Science*, *208*, 47–57.
- Bennett, W. F., Sapay, N., & Tieleman, D. P. (2014). Atomistic simulations of pore formation and closure in lipid bilayers. *Biophysical Journal*, *106*, 210–219.
- Bingham, R. J., Smye, S. W., & Olmsted, P. D. (2015). Dynamics of an asymmetric bilayer lipid membrane in a viscous solvent. *Europhysics Letters*, *111*, 18004.

- Bloom, M., & Evans, E. (1991). Observations of surface undulations on the mesoscopic length scale by NMR. In L. Peliti (Ed.), *Biologically inspired physics* (pp. 137–147). New York: Plenum.
- Bloom, M., Evans, E., & Mouritsen, O. G. (1991). Physical properties of the fluid lipid-bilayer component of cell membranes: A perspective. *Quarterly Reviews of Biophysics*, 24, 293–397.
- Brogden, K. A. (2005). Antimicrobial peptides: Pore formers or metabolic inhibitors in bacteria? *Nature Reviews Microbiology*, 3, 238–250.
- Brown, M. F. (1979). Deuterium relaxation and molecular dynamics in lipid bilayers. *Journal of Magnetic Resonance*, 35, 203–215.
- Brown, M. F. (1982). Theory of spin-lattice relaxation in lipid bilayers and biological membranes. ^2H and ^{14}N quadrupolar relaxation. *The Journal of Chemical Physics*, 77, 1576–1599.
- Brown, M. F. (1984). Unified picture for spin-lattice relaxation of lipid bilayers and biomembranes. *The Journal of Chemical Physics*, 80, 2832–2836.
- Brown, M. F. (1994). Modulation of rhodopsin function by properties of the membrane bilayer. *Chemistry and Physics of Lipids*, 73, 159–180.
- Brown, M. F. (1996). Membrane structure and dynamics studied with NMR spectroscopy. In K. M. Merz Jr., & B. Roux (Eds.), *Biological membranes. A molecular perspective from computation and experiment* (pp. 175–252). Basel: Birkhäuser.
- Brown, M. F. (2012). Curvature forces in membrane lipid–protein interactions. *Biochemistry*, 51, 9782–9795.
- Brown, M. F. (2017). Soft matter in lipid–protein interactions. *Annual Review of Biophysics*, 46, 379–410.
- Brown, M. F., & Chan, S. I. (1996). Bilayer membranes: Deuterium & carbon-13 NMR. In D. M. Grant, & R. K. Harris (Eds.), Vol. 2. *Encyclopedia of nuclear magnetic resonance* (pp. 871–885). New York: John Wiley & Sons.
- Brown, D., & London, E. (1998). Functions of lipid rafts in biological membranes. *Annual Review of Cell and Developmental Biology*, 14, 111–136.
- Brown, M. F., Ribeiro, A. A., & Williams, G. D. (1983). New view of lipid bilayer dynamics from ^2H and ^{13}C NMR relaxation time measurements. *Proceedings of the National Academy of Sciences of the United States of America*, 80, 4325–4329.
- Brown, M. F., & Seelig, J. (1978). Influence of cholesterol on the polar region of phosphatidylcholine and phosphatidylethanolamine bilayers. *Biochemistry*, 17, 381–384.
- Brown, M. F., Thurmond, R. L., Dodd, S. W., Otten, D., & Beyer, K. (2001). Composite membrane deformation on the mesoscopic length scale. *Physical Review E*, 64, 010901.
- Brown, M. F., Thurmond, R. L., Dodd, S. W., Otten, D., & Beyer, K. (2002). Elastic deformation of membrane bilayers probed by deuterium NMR relaxation. *Journal of the American Chemical Society*, 124, 8471–8484.
- Carrillo, J.-M. Y., Katsaras, J., Sumpter, B. G., & Ashkar, R. (2017). A computational approach for modeling neutron scattering data from lipid bilayers. *Journal of Chemical Theory and Computation*, 13, 916–925.
- Chakraborty, S., Doktorova, M., Molugu, T. R., Heberle, F. A., Scott, H. L., Dzikovski, B., et al. (2020). How cholesterol stiffens unsaturated lipid membranes. *Proceedings of the National Academy of Sciences of the United States of America*, 117, 21896–21905.
- Cornelius, F. (2001). Modulation of Na,K-ATPase and Na-ATPase activity by phospholipids and cholesterol. I. Steady-state kinetics. *Biochemistry*, 40, 8842–8851.
- Corvera, E., Mouritsen, O. G., Singer, M. A., & Zuckermann, M. J. (1992). The permeability and the effect of acyl-chain length for phospholipid bilayers containing cholesterol: Theory and experiment. *Biochimica et Biophysica Acta*, 1107, 261–270.
- Craig, M., Yarrarapu, S. N. S., & Dimri, M. (2021). *Biochemistry, cholesterol*. Treasure Island (FL): StatPearls Publishing LLC.
- De Mel, J. U., Gupta, S., Perera, R. M., Ngo, L. T., Zolnierczuk, P., Bleuel, M., et al. (2020). Influence of external NaCl salt on membrane rigidity of neutral DOPC vesicles. *Langmuir*, 36, 9356–9367.
- De Mel, J. U., Gupta, S., Willner, L., Allgaier, J., Stingaciu, L. R., Bleuel, M., et al. (2021). Manipulating phospholipid vesicles at the nanoscale: A transformation from unilamellar to multilamellar by an *n*-alkyl-poly(ethylene oxide). *Langmuir*, 37, 2362–2375.
- de Meyer, F. J. M., Rodgers, J. M., Willems, T. F., & Smit, B. (2010). Molecular simulation of the effect of cholesterol on lipid-mediated protein-protein interactions. *Biophysical Journal*, 99, 3629–3638.
- Dimova, R. (2014). Recent developments in the field of bending rigidity measurements on membranes. *Advances in Colloid and Interface Science*, 208, 225–234.
- Doktorova, M., Harries, D., & Khelashvili, G. (2017). Determination of bending rigidity and tilt modulus of lipid membranes from real-space fluctuation analysis of molecular dynamics simulations. *Physical Chemistry Chemical Physics*, 19, 16806–16818.

- Doktorova, M., Heberle, F. A., Kingston, R. L., Khelashvili, G., Cuendet, M. A., Wen, Y., et al. (2017). Cholesterol promotes protein binding by affecting membrane electrostatics and solvation properties. *Biophysical Journal*, *113*, 2004–2015.
- Doktorova, M., Heberle, F. A., Marquardt, D., Rusinova, R., Sanford, R. L., Peyear, T. A., et al. (2019). Gramicidin increases lipid flip-flop in symmetric and asymmetric lipid vesicles. *Biophysical Journal*, *116*, 860–873.
- Doktorova, M., LeVine, M. V., Khelashvili, G., & Weinstein, H. (2019). A new computational method for membrane compressibility: Bilayer mechanical thickness revisited. *Biophysical Journal*, *116*, 487–502.
- Duwe, H. P., Kaes, J., & Sackmann, E. (1990). Bending elastic moduli of lipid bilayers: Modulation by solutes. *Journal de Physique (Paris)*, *51*, 945–961.
- Evans, E., & Rawicz, W. (1990). Entropy-driven tension and bending elasticity in condensed-fluid membranes. *Physical Review Letters*, *64*, 2094–2097.
- Farago, B. (1999). Recent neutron spin-echo developments at the ILL (IN11 and IN15). *Physica B*, *267–268*, 270–276.
- Farago, B., Falus, P., Hoffmann, I., Gradzielski, M., Thomas, F., & Gomez, C. (2015). The IN15 upgrade. *Neutron News*, *26*, 15–17.
- Gracià, R. S., Bezlyepkina, N., Knorr, R. L., Lipowsky, R., & Dimova, R. (2010). Effect of cholesterol on the rigidity of saturated and unsaturated membranes: Fluctuation and electrodeformation analysis of giant vesicles. *Soft Matter*, *6*, 1472–1482.
- Gupta, S., De Mel, J. U., Perera, R. M., Zolnierczuk, P., Bleuel, M., Faraone, A., et al. (2018). Dynamics of phospholipid membranes beyond thermal undulations. *Journal of Physical Chemistry Letters*, *9*, 2956–2960.
- Gupta, S., De Mel, J. U., & Schneider, G. J. (2019). Dynamics of liposomes in the fluid phase. *Current Opinion in Colloid & Interface Science*, *42*, 121–136.
- Gupta, S., & Schneider, G. J. (2020). Modeling the dynamics of phospholipids in the fluid phase of liposomes. *Soft Matter*, *16*, 3245–3256.
- Hladky, S. B., & Gruen, D. W. (1982). Thickness fluctuations in black lipid membranes. *Biophysical Journal*, *38*, 251–258.
- Hoffmann, I., Michel, R., Sharp, M., Holderer, O., Appavou, M. S., Polzer, F., et al. (2014). Softening of phospholipid membranes by the adhesion of silica nanoparticles—as seen by neutron spin-echo (NSE). *Nanoscale*, *6*, 6945–6952.
- Holderer, O., & Ivanova, O. (2015). J-NSE: Neutron spin echo spectrometer. *Journal of Large-Scale Research Facilities*, *1*, A11.
- Israelachvili, J. N., & Wennerström, H. (1992). Entropic forces between amphiphilic surfaces in liquids. *The Journal of Physical Chemistry*, *96*, 520–531.
- Johner, N., Harries, D., & Khelashvili, G. (2014). Curvature and lipid packing modulate the elastic properties of lipid assemblies: Comparing HII and lamellar phases. *Journal of Physical Chemistry Letters*, *5*, 4201–4206.
- Johner, N., Harries, D., & Khelashvili, G. (2016). Erratum to: Implementation of a methodology for determining elastic properties of lipid assemblies from molecular dynamics simulations. *BMC Bioinformatics*, *17*, 236.
- Johner, N., Harries, D., & Khelashvili, G. (2016). Implementation of a methodology for determining elastic properties of lipid assemblies from molecular dynamics simulations. *BMC Bioinformatics*, *17*, 161.
- Katsaras, J., & Gutberlet, T. (2001). *Lipid bilayers: Structure and interactions*. Berlin, Heidelberg: Springer-Verlag.
- Kelley, E. G., Butler, P. D., Ashkar, R., Bradbury, R., & Nagao, M. (2020). Scaling relationships for the elastic moduli and viscosity of mixed lipid membranes. *Proceedings of the National Academy of Sciences of the United States of America*, *117*, 23365–23373.
- Khelashvili, G., & Harries, D. (2013). How cholesterol tilt modulates the mechanical properties of saturated and unsaturated lipid membranes. *The Journal of Physical Chemistry*, *117*, 2411–2421.
- Khelashvili, G., Johner, N., Zhao, G., Harries, D., & Scott, H. L. (2014). Molecular origins of bending rigidity in lipids with isolated and conjugated double bonds: The effect of cholesterol. *Chemistry and Physics of Lipids*, *178*, 18–26.
- Khondker, A., Alsop, R. J., Dhaliwal, A., Saem, S., Moran-Mirabal, J. M., & Rheinstädter, M. C. (2017). Membrane cholesterol reduces polymyxin B nephrotoxicity in renal membrane analogs. *Biophysical Journal*, *113*, 2016–2028.
- Klose, C., Surma, M. A., & Simons, K. (2013). Organellar lipidomics—Background and perspectives. *Current Opinion in Cell Biology*, *25*, 406–413.
- Krause, M. R., & Regen, S. L. (2014). The structural role of cholesterol in cell membranes: From condensed bilayers to lipid rafts. *Accounts of Chemical Research*, *47*, 3512–3521.
- Kučerka, N., Nieh, M. P., & Katsaras, J. (2011). Fluid phase lipid areas and bilayer thicknesses of commonly used phosphatidylcholines as a function of temperature. *Biochimica et Biophysica Acta*, *1808*, 2761–2771.
- Kuroda, Y., Nasu, H., Fujiwara, Y., & Nakagawa, T. (2000). Orientations and locations of local anesthetics benzocaine and butamben in phospholipid membranes as studied by ^2H NMR spectroscopy. *The Journal of Membrane Biology*, *177*, 117–128.

- Lee, J. H., Choi, S. M., Doe, C., Faraone, A., Pincus, P. A., & Kline, S. R. (2010). Thermal fluctuation and elasticity of lipid vesicles interacting with pore-forming peptides. *Physical Review Letters*, *105*, 038101.
- Leeb, F., & Maibaum, L. (2018). Spatially resolving the condensing effect of cholesterol in lipid bilayers. *Biophysical Journal*, *115*, 2179–2188.
- Leftin, A., Xu, X., & Brown, M. F. (2014). Phospholipid bilayer membranes: Deuterium and carbon-13 NMR spectroscopy. *eMagRes*, *3*, 199–214.
- Liu, S.-L., Sheng, R., Jung, J. H., Wang, L., Stec, E., O'Connor, M. J., et al. (2017). Orthogonal lipid sensors identify transbilayer asymmetry of plasma membrane cholesterol. *Nature Chemical Biology*, *13*, 268–274.
- Martinez, G. V., Dykstra, E. M., Lope-Piedrafita, S., Job, C., & Brown, M. F. (2002). NMR elastometry of fluid membranes in the mesoscopic regime. *Physical Review E*, *66*, 050902.
- Matsuzaki, K. (1999). Why and how are peptide–lipid interactions utilized for self-defense? Magainins and tachyplesins as archetypes. *Biochimica et Biophysica Acta*, *1462*, 1–10.
- Matsuzaki, K., Sugishita, K., Fujii, N., & Miyajima, K. (1995). Molecular basis for membrane selectivity of an antimicrobial peptide, magainin 2. *Biochemistry*, *34*, 3423–3429.
- Maxfield, F. R., & van Meer, G. (2010). Cholesterol, the central lipid of mammalian cells. *Current Opinion in Cell Biology*, *22*, 422–429.
- Meher, G., Bhattacharjya, S., & Chakraborty, H. (2019). Membrane cholesterol modulates oligomeric status and peptide-membrane interaction of severe acute respiratory syndrome coronavirus fusion peptide. *The Journal of Physical Chemistry B*, *123*, 10654–10662.
- Mezei, F. (1972). Neutron spin echo: A new concept in polarized thermal neutron techniques. *Zeitschrift für Physik*, *255*, 146–160.
- Mezei, F., Pappas, C., & Gutberlet, T. (2002). *Neutron spin echo spectroscopy basics, trends and applications*. Berlin: Springer-Verlag.
- Miller, I. R. (1984). Energetics of fluctuation in lipid bilayer thickness. *Biophysical Journal*, *45*, 643–644.
- Molugu, T. R., & Brown, M. F. (2016). Cholesterol-induced suppression of membrane elastic fluctuations at the atomic level. *Chemistry and Physics of Lipids*, *199*, 39–51.
- Molugu, T. R., Lee, S., & Brown, M. F. (2017). Concepts and methods of solid-state NMR spectroscopy applied to biomembranes. *Chemical Reviews*, *117*, 12087–12132.
- Molugu, T. R., Mallikarjunaiah, K. J., Job, C., & Brown, M. F. (2012). Hydration-mediated slow dynamics in phospholipid membranes. *Biophysical Journal*, *102*, 389A–390A.
- Molugu, T. R., Mallikarjunaiah, K. J., Job, C., & Brown, M. F. (2013). Suppression of cooperative motions in phospholipid membranes by osmotic stress: Deuterium NMR relaxation study. *Biophysical Journal*, *104*, 81A.
- Monkenbusch, M., & Richter, D. (2007). High resolution neutron spectroscopy—A tool for the investigation of dynamics of polymers and soft matter. *Comptes Rendus Physique*, *8*, 845–864.
- Monkenbusch, M., Schätzler, R., & Richter, D. (1997). The Jülich neutron spin-echo spectrometer—Design and performance. *Nuclear Instruments and Methods in Physics Research, Section A*, *399*, 301–323.
- Mouritsen, O. G., & Zuckermann, M. J. (2004). What's so special about cholesterol? *Lipids*, *39*, 1101–1113.
- Movileanu, L., Popescu, D., Ion, S., & Popescu, A. I. (2006). Transbilayer pores induced by thickness fluctuations. *Journal of Mathematical Biology*, *68*, 1231–1255.
- Nagao, M., Kelley, E. G., Ashkar, R., Bradbury, R., & Butler, P. D. (2017). Probing elastic and viscous properties of phospholipid bilayers using neutron spin echo spectroscopy. *Journal of Physical Chemistry Letters*, *8*, 4679–4684.
- Nagle, J. F., & Tristram-Nagle, S. (2000). Structure of lipid bilayers. *Biochimica et Biophysica Acta*, *1469*, 159–195.
- Nevezorov, A. A., & Brown, M. F. (1997). Dynamics of lipid bilayers from comparative analysis of ^2H and ^{13}C nuclear magnetic resonance relaxation data as a function of frequency and temperature. *The Journal of Chemical Physics*, *107*, 10288–10310.
- Nevezorov, A. A., Trouard, T. P., & Brown, M. F. (1998). Lipid bilayer dynamics from simultaneous analysis of orientation and frequency dependence of deuterium spin-lattice and quadrupolar order relaxation. *Physical Review E*, *58*, 2259–2281.
- Niggemann, G., Kummrow, M., & Helfrich, W. (1995). The bending rigidity of phosphatidylcholine bilayers: Dependences on experimental method, sample cell sealing and temperature. *Journal de Physique II (Paris)*, *5*, 413–425.
- Ohl, M., Monkenbusch, M., Arend, N., Kozielski, T., Vehres, G., Tiemann, C., et al. (2012). The spin-echo spectrometer at the spallation neutron source (SNS). *Nuclear Instruments and Methods in Physics Research*, *696*, 85–99.

- Orsia, M., & Essex, J. W. (2010). Permeability of drugs and hormones through a lipid bilayer: Insights from dual-resolution molecular dynamics. *Soft Matter*, 6, 3797–3808.
- Pan, J., Mills, T. T., Tristram-Nagle, S., & Nagle, J. F. (2008). Cholesterol perturbs lipid bilayers nonuniversally. *Physical Review Letters*, 100, 198103.
- Pan, J., Tristram-Nagle, S., & Nagle, J. F. (2009). Effect of cholesterol on structural and mechanical properties of membranes depends on lipid chain saturation. *Physical Review E*, 80, 021931.
- Prasad, V. R., & Bukrinsky, M. I. (2014). New clues to understanding HIV nonprogressors: Low cholesterol blocks HIV trans infection. *mBio*, 5, e01396–14.
- Rawicz, W., Olbrich, K. C., McIntosh, T., Needham, D., & Evans, E. (2000). Effect of chain length and unsaturation on elasticity of lipid bilayers. *Biophysical Journal*, 79, 328–339.
- Reif, B., Ashbrook, S. E., Emsley, L., & Hong, M. (2021). Solid-state NMR spectroscopy. *Nature Reviews Disease Primers*, 2, 1–23.
- Rose, M. E. (1957). *Elementary theory of angular momentum*. New York: John Wiley & Sons.
- Rosov, N., Rathgeber, S., & Monkenbusch, M. (1999). Neutron spin echo spectroscopy at the NIST Center for Neutron Research. In P. Cebe, B. S. Hsiao, & D. J. Lohse (Eds), *Scattering from polymers. Characterization by X-rays, neutrons, and light* (Vol. 739, pp. 103–116). American Chemical Society.
- Sandhu, G., Booth, V., & Morrow, M. R. (2020). Role of charge in lipid vesicle binding and vesicle surface saturation by gaduscidin-1 and gaduscidin-2. *Langmuir*, 36, 9867–9877.
- Schachter, I., Allolio, C., Khelashvili, G., & Harries, D. (2020). Confinement in nanodiscs anisotropically modifies lipid bilayer elastic properties. *The Journal of Physical Chemistry B*, 124, 7166–7175.
- Sharma, V. K., Mamontov, E., Ohl, M., & Tyagi, M. (2017). Incorporation of aspirin modulates the dynamical and phase behavior of the phospholipid membrane. *Physical Chemistry Chemical Physics*, 19, 2514–2524.
- Sheng, R., Chen, Y. H., Gee, H. Y., Stec, E., Melowic, H. R., Blatner, N. R., et al. (2012). Cholesterol modulates cell signaling and protein networking by specifically interacting with PDZ domain-containing scaffold proteins. *Nature Communications*, 3, 1–9.
- Sherman, P. J., Jackway, R. J., Gehman, J. D., Praporski, S., McCubbin, G. A., Mechler, A., et al. (2009). Solution structure and membrane interactions of the antimicrobial peptide fallaxidin 4.1a: An NMR and QCM study. *Biochemistry*, 48, 11892–11901.
- Siminovitch, D. J., Brown, M. F., & Jeffrey, K. R. (1984). ^{14}N NMR of lipid bilayers: Effects of ions and anesthetics. *Biochemistry*, 23, 2412–2420.
- Simons, K., & Gerl, M. J. (2010). Revitalizing membrane rafts: New tools and insights. *Nature Reviews Molecular Cell Biology*, 11, 688–699.
- Simons, K., & Ikonen, E. (2000). How cells handle cholesterol. *Science*, 290, 1721–1726.
- Su, Y., Li, S., & Hong, M. (2013). Cationic membrane peptides: Atomic-level insight of structure–activity relationships from solid-state NMR. *Amino Acids*, 44, 821–833.
- Sun, X., & Whittaker, G. R. (2003). Role for influenza virus envelope cholesterol in virus entry and infection. *Journal of Virology*, 77, 12543–12551.
- Thewalt, J. L., & Cushley, R. J. (1987). Phospholipid/cholesterol membranes containing *n*-alkanols: A ^2H -NMR study. *Biochimica et Biophysica Acta*, 905, 329–338.
- Trouard, T. P., Nevzorov, A. A., Alam, T. M., Job, C., Zajicek, J., & Brown, M. F. (1999). Influence of cholesterol on dynamics of dimyristoylphosphatidylcholine as studied by deuterium NMR relaxation. *The Journal of Chemical Physics*, 110, 8802–8818.
- Turner, G. L., & Oldfield, E. (1979). Effect of a local anaesthetic on hydrocarbon chain order in membranes. *Nature*, 277, 669–670.
- van Hove, L. (1954). Correlations in space and time and Born approximation scattering in systems of interacting particles. *Physical Review*, 95, 249–262.
- Vermeer, L. S., De Groot, B. L., Reat, V., Milon, A., & Czaplicki, J. (2007). Acyl chain order parameter profiles in phospholipid bilayers: Computation from molecular dynamics simulations and comparison with ^2H NMR experiments. *European Biophysics Journal*, 36, 919–931.
- Watson, M. C., & Brown, F. L. (2010). Interpreting membrane scattering experiments at the mesoscale: The contribution of dissipation within the bilayer. *Biophysical Journal*, 98, L9–L11.
- Woodka, A. C., Butler, P. D., Porcar, L., Farago, B., & Nagao, M. (2012). Lipid bilayers and membrane dynamics: Insight into thickness fluctuations. *Physical Review Letters*, 109, 058102.

- Xu, X., Struts, A. V., & Brown, M. F. (2014). Generalized model-free analysis of nuclear spin relaxation experiments. *eMagRes*, 3, 275–286.
- Yamada, L. N., Seto, H., Takeda, T., Nagao, M., Kawabata, Y., & Inoue, K. (2005). SAXS, SANS and NSE studies on “unbound state” in DPPC/water/CaCl₂ system. *Journal of the Physical Society of Japan*, 74, 2853–2859.
- Zaslhoff, M. (2002). Antimicrobial peptides of multicellular organisms. *Nature*, 415, 389–395.
- Zhang, X., Barraza, K. M., & Beauchamp, J. L. (2018). Cholesterol provides nonsacrificial protection of membrane lipids from chemical damage at air–water interface. *Proceedings of the National Academy of Sciences of the United States of America*, 115, 3255–3260.
- Zilman, A. G., & Granek, R. (1996). Undulations and dynamic structure factor of membranes. *Physical Review Letters*, 77, 4788–4791.